Sparse Principal Axes Statistical Deformation Models for Respiration Analysis and Classification

Jakob Wasza[1], Sebastian Bauer[1], Sven Haase[1,2], Joachim Hornegger[1,3]

[1] Pattern Recognition Lab, University of Erlangen-Nuremberg
[2] TUM Graduate School of Information Science in Health (GSISH)
[3] Erlangen Graduate School in Advanced Optical Technologies (SAOT)

BVM, Berlin, 3/22/2012

FRIEDRICH-ALEXANDER UNIVERSITÄT ERLANGEN-NÜRNBERG
TECHNISCHE FAKULTÄT

Outline

- Motivation
  - Respiratory Motion
  - Range Imaging based Surrogates
- Methods
  - Range Imaging
  - Principal Component Analysis
  - Orthomax Rotations
- Results
  - PCA vs. Varimax Rotations
  - Applications
- Conclusion and Outlook

Motivation

- Respiratory Motion
- Range Imaging based Surrogates

Motivation

- Internal movement due to respiratory motion
  - Tomographic reconstruction
  - Fractionated radiotherapy
- Gating and beam adjustment based on 1-D respiration surrogates
  - Dedicated sensors attached to the body surface
  - Non-intrusive range imaging (RI)
- Current RI-based 1-D surrogates
  - Manually selected points and regions
  - Heuristic surface partitioning
  - Global statistical models

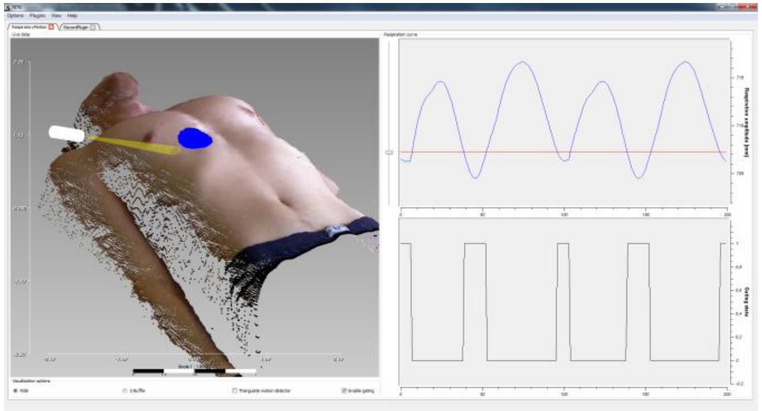

Figure: Gated radiotherapy using RI techniques.

Motivation

- Drawbacks of conventional statistical models
  - Fail to describe local deformations (e.g. thoracic and abdominal breathing)
  - Hinder an intuitive interpretation of the model's inherent variations
  - Produce invalid shapes w.r.t. the human respiration system

- Sparse axes models to produce relief
  - Relate local deformations to sparsity of the model's principal axes
  - Orthomax criterion to derive sparse principal modes of variation [1]

[1] Stegmann M.B, Sjöstrand K, Larsen R.
Sparse Modeling of Landmark and Texture Variability using the Orthomax Criterion.
In: Proc SPIE. vol. 6144; 2006. p. 61441G1-61441G.12.

Methods

- Range Imaging
- Principal Component Analysis
- Orthomax Rotations

Range Imaging

Usually denotes an ROI

- Sensor domain $\Omega : N \times M \mapsto \mathbb{R}$
- Range image $f(\boldsymbol{x}),\ \boldsymbol{x} \in \Omega$
- Linearized range image
  $$f \equiv \boldsymbol{g} = \left(f(\boldsymbol{x}_1),\ \ldots,\ f(\boldsymbol{x}_{N \cdot M})\right)^T,\ \boldsymbol{g} \in \mathbb{R}^{N \cdot M}$$
- Training data acquired at K different respiration states i
  $$\mathcal{G} = \{\boldsymbol{g}_i\}_{i=1}^{K},\ \boldsymbol{g}_i \equiv f_i$$

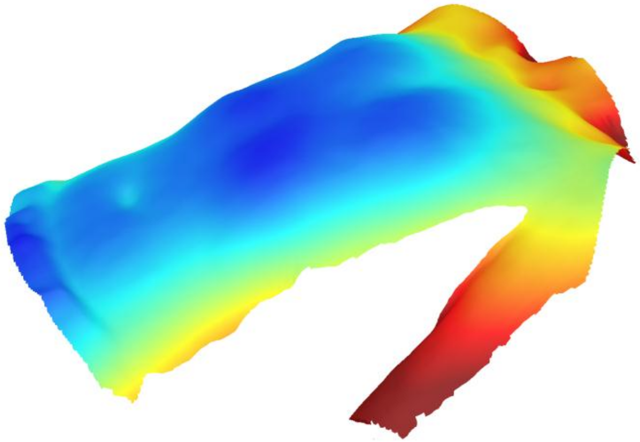

Figure: Body surface captured by the Microsoft Kinect RI device.

Principal Component Analysis (PCA)

- Configuration matrix

$$\boldsymbol{L} = [\boldsymbol{g}_1 - \overline{\boldsymbol{g}},\ \boldsymbol{g}_2 - \overline{\boldsymbol{g}},\ \ldots,\ \boldsymbol{g}_K - \overline{\boldsymbol{g}}],\ \boldsymbol{L} \in \mathbb{R}^{N \cdot M \times K},\ \overline{\boldsymbol{g}} = \sum_{i=1}^{K} \boldsymbol{g}_i$$

- Eigendecomposition and principal component basis $\boldsymbol{\Phi}$

$$\left(\boldsymbol{L}^T \boldsymbol{L}\right) \widetilde{\boldsymbol{e}}_i = \lambda_i \widetilde{\boldsymbol{e}} \qquad \boldsymbol{\Phi} = \left[\boldsymbol{L}\widetilde{\boldsymbol{e}}_1,\ \boldsymbol{L}\widetilde{\boldsymbol{e}}_2,\ \ldots,\ \boldsymbol{L}\widetilde{\boldsymbol{e}}_P\right],\ \boldsymbol{\Phi} \in \mathbb{R}^{N \cdot M \times P}$$

- Linear span of the model

Controls the modes

$$\boldsymbol{g}^* = \overline{\boldsymbol{g}} + \boldsymbol{\Phi}\boldsymbol{b},\ \boldsymbol{b} \in \mathbb{R}^P \qquad \boldsymbol{b} = \boldsymbol{\Phi}^T \left(\boldsymbol{g}^* - \overline{\boldsymbol{g}}\right)$$

- Note that PCA maximizes the variance of the input data along the basis vectors $\boldsymbol{L}\widetilde{\boldsymbol{e}}_i$.

$\longrightarrow$ Thus, global modes are obtained!

Orthomax Rotations

$$\boldsymbol{R}^T = \boldsymbol{R}^{-1},\ det(\boldsymbol{R}) = 1$$

- Optimization problem

$$\boldsymbol{R}_O = \underset{\boldsymbol{R}}{\operatorname{argmax}} \sum_{j=1}^{P} \sum_{i=1}^{N \cdot M} (\boldsymbol{\Phi R})_{ij}^4 - \frac{\gamma}{N \cdot M} \sum_{j=1}^{P} \left(\sum_{i=1}^{N \cdot M} (\boldsymbol{\Phi R})_{ij}^2 \right)^2$$

- Varimax rotation ($\gamma = 1$)

$$E\left(X^2\right) \qquad \left(E\left(X\right)\right)^2$$

$$\boldsymbol{R}_O = \underset{\boldsymbol{R}}{\operatorname{argmax}} \sum_{j=1}^{P} \left(\frac{1}{N \cdot M} \sum_{i=1}^{N \cdot M} \boldsymbol{\delta}_{ij}^2 - \left(\frac{1}{N \cdot M} \sum_{i=1}^{N \cdot M} \boldsymbol{\delta}_{ij} \right)^2 \right),\ \boldsymbol{\delta}_{i,j} = (\boldsymbol{\Phi R})_{i,j}^2$$

- Varimax rotations transform the model basis according to $\boldsymbol{\Phi}_O = \boldsymbol{\Phi R}_O$, maximizing the squared variable loadings by bringing several loadings close to zero.

$\longrightarrow$ This favors sparse modes!

Results

- PCA vs. Varimax Rotations
- Applications

Results

- Dimension reduction
  - Abdominal and thoracic breathing
  - Two separate and one joint model

Mode of variation	Abdominal	Thoracic	Joint
#1	98.4 % (98.4%)	92.7 % (92.7%)	75.3 % (75.3%)
#2	~1.0 % (99.4%)	~ 5.9 % (98.6%)	23.2 % (98.5%)
#3	< 1.0 % (99.8%)	< 1.0 % (99.4%)	~ 1.0 % (99.4%)
#4	< 1.0 % (99.9%)	< 1.0 % (99.6%)	< 1.0 % (99.6%)
Total	**99.9%**	**99.6%**	**99.6%**

Table: Variance covered by the first four modes of variation.

Results

- PCA vs. varimax rotations

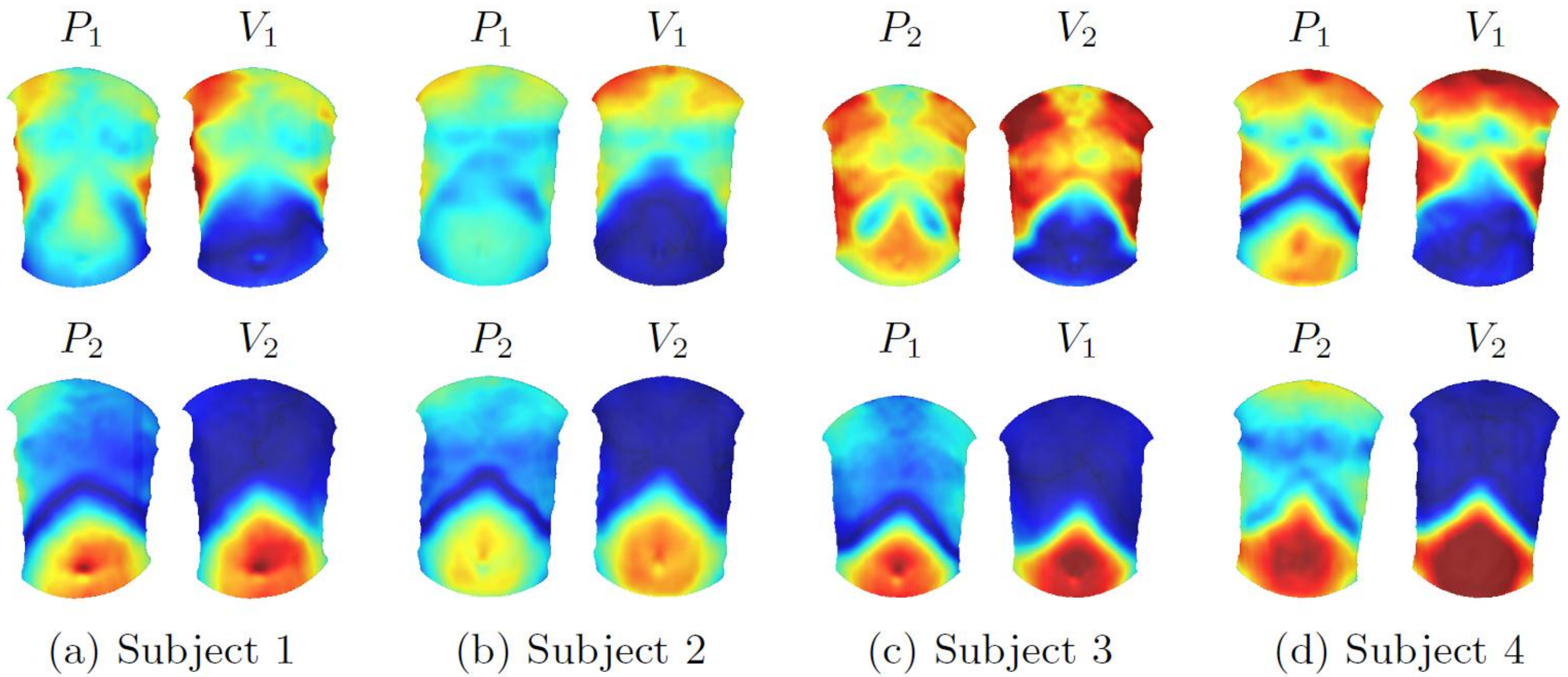

Figure: Respiratory motion patterns from statistical analysis. PCA (P) and Varimax rotations (V). Magnitude of variation is color coded from blue (low) to red (high).

Results

- Simulation of respiration states for algorithm benchmarking

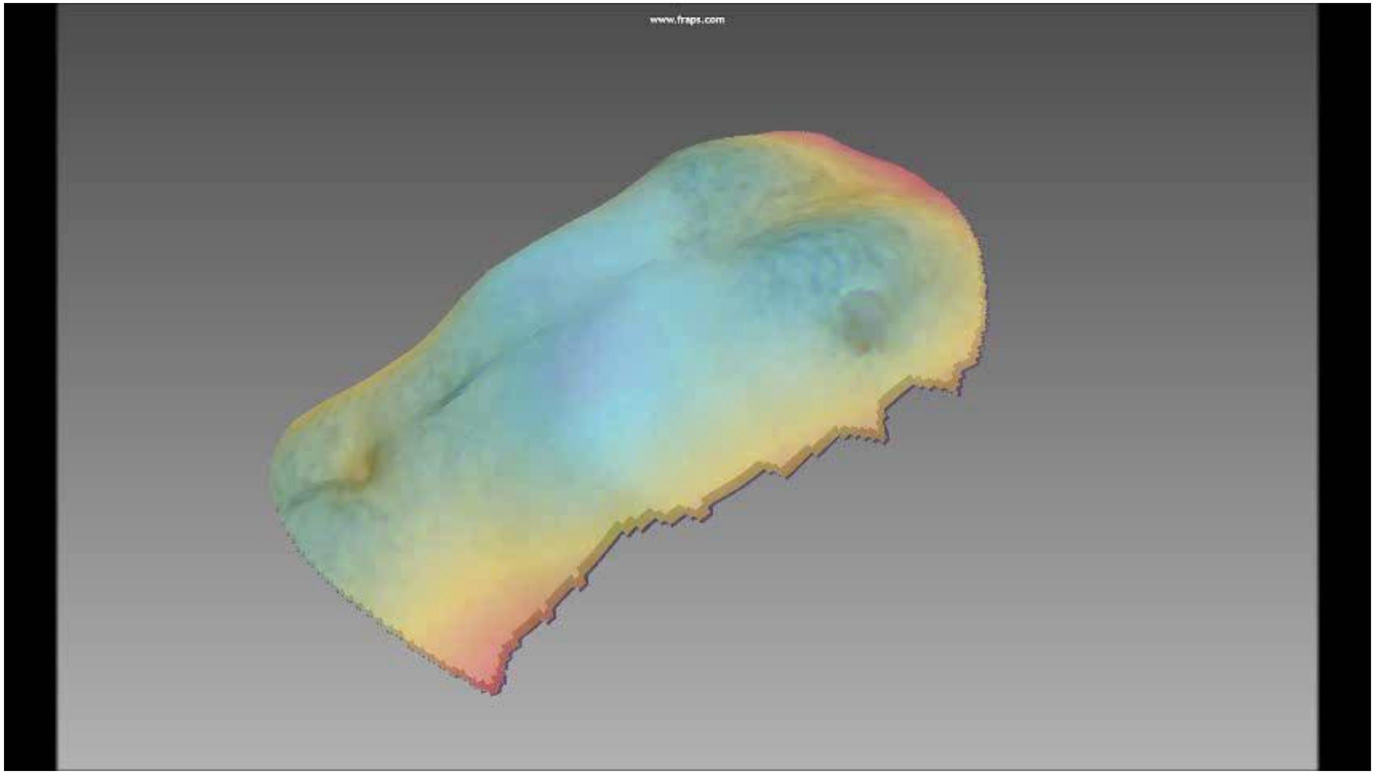

Results

- Patient specific respiration analysis and classification

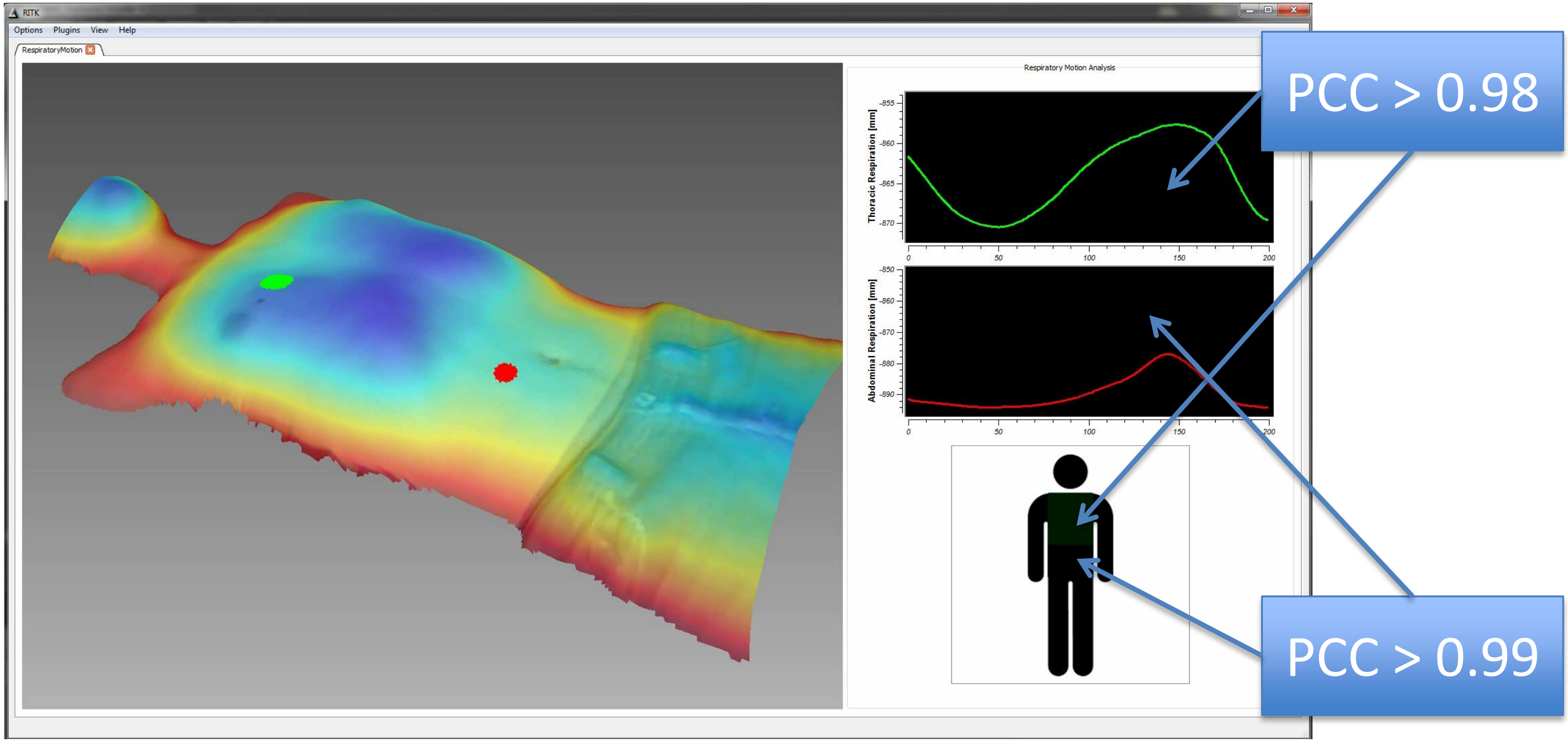

Conclusion and Outlook

Conclusions and Outlook

- Sparse principal axes for respiration analysis
  - Varimax rotations to generate sparse modes
  - Local surface deformations
  - Differentiation between thoracic and abdominal breathing

- Future work
  - Extension to 3-D point clouds
  - Non-linear techniques for model generation

Thank you for your attention!

Acknowledgements

- We gratefully acknowledge the support by the ***European Regional Development Fund*** and the ***Bayerisches Staatsministerium für Wirtschaft, Infrastruktur, Verkehr und Technologie*** in the context of the R&D program IuK Bayern under Grant No. IUK338.

- We gratefully acknowledge the Support by the ***Deutsche Forschungsgemeinschaft*** under Grant No. HO 1791/7-1 and the **Graduate School of Information Science in Health** (GSISH) and the TUM Graduate School.